All-optical synapses based on silicon microring resonators actuated by the phase change material $Ge_2Sb_2Te_5$

Hanyu Zhang[1], Linjie Zhou[1*], Jian Xu[1], Liangjun Lu[1], and Jianping Chen[1], B. M. A. Rahman[2]
[1]*State Key Laboratory of Advanced Optical Communication Systems and Networks, Department of Electronic Engineering, Shanghai Jiao Tong University, Shanghai, China*
[2]*Department of Electrical and Electronic Engineering, City, University of London, London, U.K.*
[*]*ljzhou@sjtu.edu.cn*

Abstract: We demonstrate silicon microring resonators integrated with $Ge_2Sb_2Te_5$ material that can be used as all-optical synapses for neuromorphic computing. Synaptic plasticity is investigated with different resonator coupling conditions.
OCIS codes: 160.2900 Optical storage materials; 160.3130 Integrated optics materials; 130.3120 Integrated optics devices.

1. Introduction

The human brain consists of ~10^{11} neurons and an extremely large number of synapses acting as a highly complex interconnection network among the neurons [1]. Neuromorphic computation is implemented by integrating the inputs coming from other neurons and generating spikes as a result. The synapses contribute to the computation by changing their connection strength as a result of neuronal activity, which is known as synaptic plasticity [2]. Synaptic plasticity is the mechanism that is believed to underlie learning and memory of the biological brain. Several electronic devices based on phase change materials (PCMs), ferroelectric switches and carbon nanotubes have been explored to obtain synaptic functions [3].

In this paper, we demonstrate all-optical synapses based on $Ge_2Sb_2Te_5$ (GST)-loaded microring resonators in which the optical transmission can be gradually increased (long-term potentiation, LTP) or decreased (long-term depression, LTD) due to phase change of GST in response to neuron spikes.

2. Structure and principle

The concept of a photonic synapse is shown schematically in Fig. 1(a). A silicon microring resonator integrated with a small piece of GST material on top of the ring waveguide working as a synapse is connected with a pre-neuron and a post-neuron. An off-chip optical circulator is used for two purposes: connecting the output of the synapse with the post-neuron, and applying optical pulses to alter the synaptic weight. The optical transmission from the pre-neuron can be measured, with the transmission level dependent on the synaptic weight. The coupling regime in which the microring resonator is located is determined by the coupler length L_c, the GST length L_{GST}, and the crystallization degree of GST. The coupling condition affects the synaptic plasticity, producing LTP, LTD or both effects.

Fig. 1(b) illustrates the structure of the active region of the photonic synapse. A 15-nm-thick GST layer and a 10-nm-thick indium tin oxide (ITO) layer with a length of L_{GST} are placed on top of the single-mode silicon waveguide. When the GST changes from the amorphous state to the crystalline state, the hybrid waveguide exhibits a larger propagation constant and a higher optical absorption loss. Thus, the optical transmission through the GST-loaded waveguide can be efficiently modulated by changing the GST phase state. The resonance effect of the microring resonator amplifies the small change to detectable multiple levels.

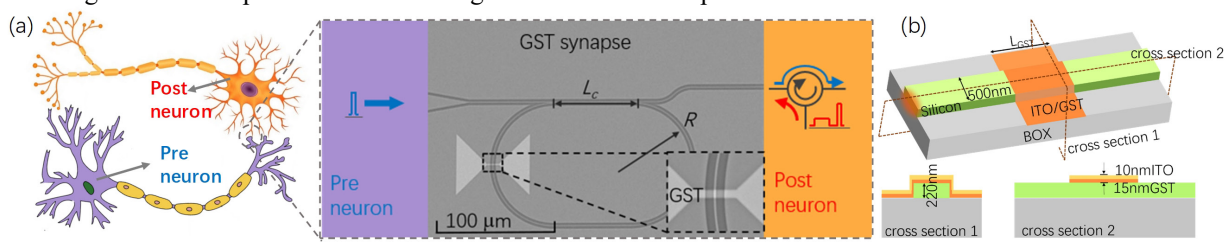

Fig. 1. (a) Structure of the neuron and synapse. Inset: illustration of the photonic synapse and the scanning electron microscope image of the device. (b) Schematic overview of the GST-loaded silicon waveguide in the photonic synapse.

3. Results and Discussion

We designed three photonic synaptic structures (synapses I, II, III) based on microring resonators. The fabrication process and experimental setup have previously been demonstrated in Ref. [4]. The first microring

resonator (synapse I) incorporates a 1-μm-long GST. It works in the over-coupling regime for amorphous state and near the critical-coupling regime for the crystalline state. Therefore, the amorphous state exhibits a much lower resonance extinction ratio (ER) than the crystalline state. Fig. 2(a) shows the normalized spectra for two phase change cycles (two crystalline states and two amorphous states). The inset illustrates the magnified spectra. The good overlap of the two spectra in each state indicates the excellent repeatability of the GST crystallization and re-amorphization processes. Fig. 2(d) shows the time response of the output transmission at a resonance wavelength of 1549.8 nm. The crystallization of GST was induced by eleven identical optical pulses with a width of 40 ns (17.5 mW peak power) at the 1559.45 nm resonance wavelength. Each of these pulses initiated partial crystallization of GST. Subsequently, the re-amorphization was induced by a single pulse with a width of 20 ns (52 mW peak power) at the same wavelength. As long as the reset pulse energy is sufficiently large, the GST in an arbitrary intermediate state can always return to the original amorphous state. In this synapse, the crystallization of GST produces the synaptic LTD effect (weight decreasing).

In the second microring resonator (synapse II), we increased the GST length to 2 μm so that the resonator works near the critical coupling regime for the amorphous state and in the under-coupling regime for the crystalline state. In this case, the amorphous state exhibits a much higher ER than the crystalline state. Figs. 2(b) and 2(e) show the static and dynamic responses for two phase change cycles in synapse II, respectively. Unlike synapse I, the crystallization process of synapse II produces the synaptic LTP effect (weight increasing).

It should be noted that the LTP and LTD effects can only be implemented separately in both synapses I and II, because the resonances cycle between two coupling regimes upon phase change. To realize both effects in one device, we designed the third microring resonator device (synapse III) with an increased GST length of 3 μm. For a longer GST, the crystallization process exhibits higher losses and more redshifts. The coupling length is also increased so that three coupling regimes can all be observed in the 1500-1600 nm wavelength range (Fig. 3(c)). Near the 1545 nm (1585 nm) wavelength, the crystallization process produces the LTP (LTD) effect. Near the 1556 nm wavelength, the coupling of the microring resonator changes from the over-coupling to the critical coupling and then to the under-coupling during crystallization of GST. As a result, the transmission level first drops and then rises, as shown in Fig. 3(f). It proves that both the LTP and LTD effects can be generated at the same wavelength by properly setting the initial coupling condition.

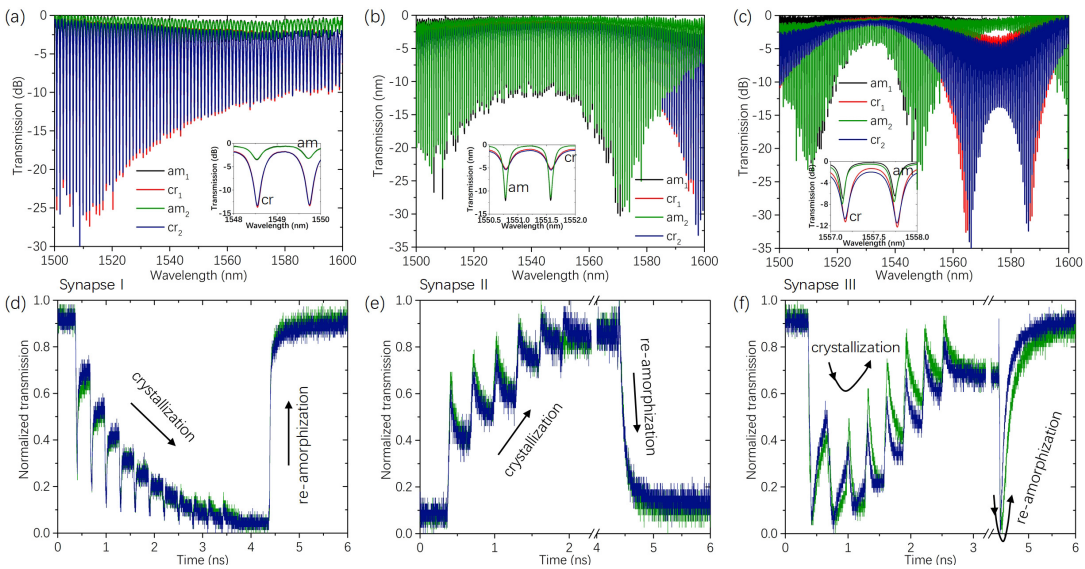

Fig. 2. (a-c) Measured transmission spectra of the all-optical synaptic devices over two phase-change cycles for (a) synapse I, (b) synapse II, and (c) synapse III. (d-f) Temporal responses of the synaptic devices when a sequence of crystallization pulses followed by a single re-amorphization pulse are applied to (d) synapse I, (e) synapse II, and (f) synapse III. The temporal trances were measured twice, showing its good repeatability.

4. References

[1] D. A. Drachman, "Do we have brain to spare?," Neurology **64**, 2004-2005 (2005).
[2] D. Kuzum, S. Yu, and H. S. Wong, "Synaptic electronics: materials, devices and applications," Nanotechnology **24**, 382001 (2013).
[3] Z. Cheng, C. Ríos, W. H. P. Pernice, C. D. Wright, and H. Bhaskaran, "On-chip photonic synapse," Sci. Adv. **3**(2017).
[4] H. Zhang, "All-optical non-volatile tuning of an AMZI-coupled ring resonator with GST phase-change material," Opt. Lett. **43**, 5539-5542 (2018).